Bending Collapse of Closed-hat-section Beams. Part II: Theoretical Model Modification and Validation

Hafizan Hashim
Amir Radzi Ab.Ghani
Wahyu Kuntjoro
Faculty of Mechanical Engineering,
Universiti Teknologi MARA, 40450 Shah Alam, Malaysia

ABSTRACT

This is the second part of the study on the bending collapse of closed-hat-section beams. This part presents an attempt to modify an existing theoretical model to predict the bending collapse mechanism and the bending response of closed-hat-section beams subject to pure bending. Previous Kecman collapse model is the main reference in the present study. According to Kecman, bending collapse of rectangular tubes exhibited so called 'hinge mechanism' on the compression flange but no significant plastic deformation was observed on the tensile side of the flange. Similarly when a closed-hat-section is bent inward, the yield line due to tensile has less influence on the overall plastic deformation. A failure mechanism consisting of stationary and rolling pastic hinge lines to produce an analytical solution using limit analysis techniques is proposed. In order to validate the analytical solution, a series of finite element analysis on pure bending of closed-hat-section beams is demonstrated. The resulting moment-rotation characterisitcs are compared with modified Kecman analytical model. Good agreement is achieved through the comparison, and the derived analytical model is therefore validated.

Keywords: *Hinge Mechanism, Finite Element, Hat-section, Bending*

Introduction

Over the past few decades, many studies have been reported on the structural collapse of thin-walled members under axial load and many efforts have been made to improve their crashworthiness. Despite these enormous works, axial progressive collapse succeeded only in laboratory and fails in the real crash.

ISSN 1823-5514, eISSN 2550-164X
Received for review: 2016-11-05
Accepted for publication: 2016-11-10
Published: 2017-06-01

It was reported that almost 90% of structural members involved in an accident failed in bending collapse mode. Meanwhile, among vehicular structures, closed-hat-section is known as a generic form used for steel profiles. It is designed for protection of occupants as well as other involving assets against impact loads. Therefore, it is essential to study the bending behavior of closed-hat-section beams so as to improve its design.

The first theoretical model for this problem was produced by Kecman [1]. Kecman (1983) proposed a collapse mechanism and derived the equations which relate to the hinge moment and associated angle of rotation. This simple failure mechanism involves stationary and moving plastic hinge lines. For the whole range of sections, good agreement between theoretical predictions and experimental results was achieved. Cimpoeru and Murray [2] experimentally studied the moment-rotation properties of thin-walled square tubes under large deflection pure bending. The results showed good agreement with existing analytical predictions developed by Kecman [1]. Another bending collapse mechanism developed for an axially loaded column was proposed by Wierzbicki *et al.* [3]. The concept of a super-folding element was extended to the case of bending and combined bending-compression loading. The theoretical models were developed and validated using numerical calculations of a square prismatic column. Kim and Reid [4] proposed a new kinematically admissible folding mechanism to predict bending collapse. It closely resembles Kecman's model with inclusion of some in-plane deformation and introduced two additional free parameters from total plastic work. The proposed analytical predictions showed good agreement with experimental data done by Kecman [1]. To replicate a generic form of steel profiles used in vehicular structures, Chen [5] studied experimentally the crushing behavior of empty and foam-filled aluminum single and double hat-section under deep bending collapse. To attain large bending angles, specimens had undergone two bending phases, 1) three-point bending up to 40°, 2) vertical compression up to 150°. Bending tests showed that the specific energy absorption (SEA) of empty section improved up to 40% by foam filling. In rollover crashes, the components in the roof structure will be subjected to large deformation bending as the roof frame collapses. Bambach *et al*. [6] experimentally studied steel spot-welded hat sections with flange perforations, subjected to deep pure bending. A theoretical procedure was then developed to determine the large deformation bending. All sections were observed to have progressively deformed in three stages; an initial elastic, an in-plane plastic, and a plastic collapse stages. On the other hand, sections slenderness affects bending moment capacity and ductility when only compact sections were developed in-plane plasticity.

The present paper re-examines the problem of uniaxial bending of closed-hat-section beams and suggests a modified collapse mechanism which is completely analytical. This theoretical approach is based on Kecman [1]

model with few modifications on additional sections. The analytical solutions were then validated via numerical approach using validated model of closed-hat-section beam in Part I of this study. The derived bending moment is compared to the results of pure bending simulation in order to verify the modified analytical. Comparison results showed good agreement and the modified analytical approach is therefore validated.

Theoretical Bending Collapse Mechanism of Closed-hat-section Beams

There are about four phases describing the actual bending collapse mechanism of a closed-hat-section beam. The first phase occurs by a protruding bulge in the webs at a fixed location without rolling deformations. It is followed by the second phase when the bulge starts to roll along yield lines GA, AK, and their symmetric counterparts as shown in Figure 1. In the next phase, the rolling deformation stops when jamming mechanism is initiated from the creation of the secondary hinge and the hinge continues to develop in the final phase of the collapse mechanism. Even though the actual collapse mechanism includes a complex combination, the deforming material is mainly concentrated along the yield lines as described by Kecman (1983) [1]. Structural continuity should be maintained at the same time, which is very difficult to achieve at any point of the theoretical model. The continuity condition will be considered at some characteristic sections only, thus ensuring that the possible discontinuities at other places are small and has negligible effect on the overall kinematics of the collapse mechanism.

The two inextensible section walls which are the undeformed segments rotate about yield lines OR and PQ at $\theta/2$ each. The collapse mechanism consists of bending deformation along the yield lines of hat (EF, GH, BC, GB, BE, HC, CF, AB, CJ, EL, GK, FM, HN) and closed-plate (OR, PQ). Rolling takes place only on the hat part that is similar to typical square

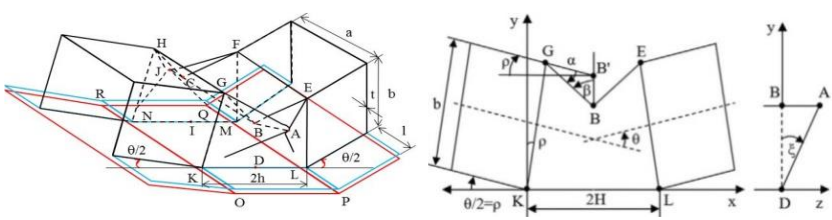

(a) (b)

Figure 1: (a) Theoretical collapse model and its (b) geometry details of a closed-hat-section beam

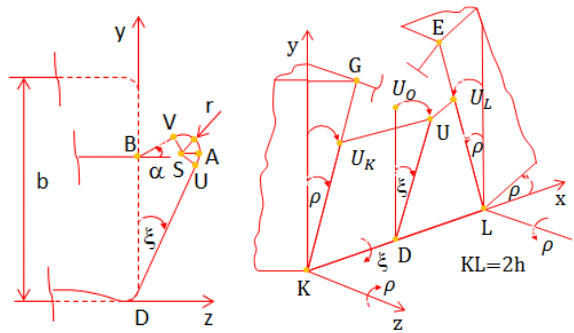

(a) (b)

Figure 2: Idealised bending collapse mechanism in the (a) web and (b) corresponding geometry detail

or rectangular section which is along the lines GA, AE, AK, AL, HJ, JF, JN and JM. The most important deformations occur in the webs as shown in cross sectional view of Figure 2 (a). Point B moves downward correspond to the compressed flange and the edges GB and EB hold the adjacent triangular segments of the web which are forced to roll along GA and EA about frictionless rollers with a radius *r* (Figure 2 (a)). Point S indicates the axis where the 'roller' passes through and is almost parallel to the line GA.

Theoretical Energy Absorbed in the Hinge

For this theoretical treatment, uniaxial bending collapse is chosen as it is almost the only mode of local collapse found in static and dynamic collapse when subjected to large deflections. Similar approach was taken by Kecman (1983), Wiezbicki *et al.* (1983), and Kim and Reid (2001) with respect to bending collapse mechanism of thin-walled tubes. To simplify the derivation work, all reinforced joints are considered to be rigid with some other additional condition and assumption to be declared later on. Complex boundary value problems are typically found in the theory of elasticity. One of the powerful tools for obtaining the approximate solutions to this problem is by using the principles of minimum potential energy and minimum complimentary energy. In nonlinear problems, plasticity is to be considered, as the exact solutions are harder to obtain than that of elastic region. The plastic strength and energy absorption problems can be tackled in two ways and both are based on the theorems of limit analysis. Limit analysis shall provide reasonably close upper and lower bounds to the true collapse load and energy absorbed.

Energy Dissipation in a Travelling Hinge

Consider a strip shown in Figure 3, with a travelling hinge defined by an arc AB of radius *r*. Suppose this hinge moves by a distance D*s* into a new

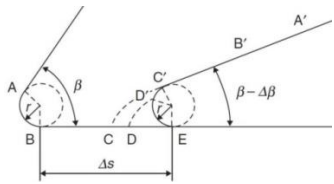

Figure 3: A strip demonstrating a traveling hinge

position, but the radius remains unchanged. For convenience, we assume that D*s* is sufficiently large that the whole arc AB is unbent into a straight segment $A'B'$. The angle β can be calculated by integrating a unit fraction of *r* over the rolled length *s*. The energy for unbending AB is then,

$$W_{AB} = \overline{AB}\frac{1}{r}m_p = m_p(\pi - \beta) \tag{1}$$

where $m_p = (\sigma_y \cdot t^2)/4$ is the fully plastic bending moment. Segment BC has been first bent into an arc of radius *r* and then unbent to a flat strip $B'C'$. Rolling deformation may be such that the rolled length $B'C'$ varies along the yield line. In such a case, it is convenient to express the rolled length as a function of the distance l from one end of the yield line. The energy required by this process along the yield line L then becomes,

$$W_{BC} = \frac{2m_p}{r}\int_0^L B'C'(l)\,\mathrm{d}l = \overline{BC}\frac{1}{r}m_p 2 \tag{2}$$

where $\overline{BC}$ is the area swept by the yield line. Similarly, for CD and DE

$$W_{CD} = \overline{CD}\frac{1}{r}m_p \quad , \quad W_{DE} = \overline{DE}\frac{1}{r}m_p. \tag{3}$$

The Compression Flange

Figure 1 shows an idealized deformation of compressed flange resulted from rotation of the hinge through an angle θ. By reusing the angle $\rho = \theta/2$, the coordinates of point G, corresponding to the hinge rotation θ are:

$$x_G = b\ \sin\rho\ ; \quad y_b = b\ \cos\rho. \tag{4}$$

Hence;

$$\beta = \text{arc sin}\frac{(h - x_G)}{GB} = \text{arc sin}\left(1 - \frac{b}{h}\sin\rho\right). \quad (5)$$

The flange walls along GH rotate relatively about z-axis at the angle of α and can be derived from the triangular GBB'. Hence:

$$\alpha = \frac{\pi}{2} - \rho - \text{arc sin}\left(1 - \frac{b}{h}\sin\rho\right). \quad (6)$$

As the hinge rotates at an angle θ about the hinge line, the plastic bending energy absorbed along yield lines EF and GH can be calculated as,

$$W_1 = W_{EF+GH} = 2\mathrm{m}_p a\left[\frac{\pi}{2} - \rho - \text{arc sin}\left(1 - \frac{b}{h}\sin\rho\right)\right] \quad (7)$$

where h is the half hinge length. The angle of relative rotation along the yield line BC is $(\pi - 2\beta)$, thus the energy absorbed becomes:

$$W_2 = W_{BC} = \mathrm{m}_p a\left[\pi - 2\ \text{arc sin}\left(1 - \frac{b}{h}\sin\rho\right)\right]. \quad (8)$$

The Web

Since the web deforms symmetrically, only one half of the section is sufficient to be considered in the calculation. The deformation includes bending along AB, BG, GK, and rolling along GA and AK. As can be seen in Figure 2, length of the yield line AB is equal to z_A and its angle of relative rotation is $(\pi - 2\beta)$, where β is known from Equation (5). The energy absorbed along AB and CJ then becomes

$$\begin{aligned} W_3 &= W_{AB+CJ} \\ &= 2m_p\Big(b\sin^2\rho - h\sin\rho \\ &\qquad + \sqrt{b\sin\rho(2h - b\sin\rho)}\ \cos\rho\Big).\Big(\pi \\ &\qquad - 2\ \text{arc sin}\left(1 - \frac{b}{h}\sin\rho\right)\Big). \end{aligned} \quad (9)$$

The angle of relative rotation along BG is $\pi/2$ and the hinge length is h. There are four yield lines under the same conditions which are BG, BE, CH, and CF and the energy absorbed for all these lines is unchanged with θ as i

$$W_4 = W_{BG+BE+CH+CF} = 4 \cdot m_p \cdot h \cdot \frac{\pi}{2} = 2 \cdot m_p \cdot h\pi. \tag{10}$$

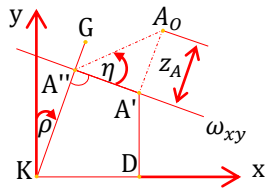

Figure 4: Detail projection geometry of yield line GK on x-y plane

Figure 4 shows detail projection geometry of the yield line GK on xy plane. η is the angle of relative rotation along yield line GK. Let a plane ω be perpendicular to GK and passing through A intersects the xy plane along the straight line ω_{xy}. Plane ω now rotates about line ω_{xy} so that point A falls into the point A_0 in xy, thus the actual angle η becomes

$$\eta = \arctan \frac{A'A_0}{A'A''}. \tag{11}$$

It is concluded that $A'A_0 = z_A$ and coordinates of point A' and B are the same. Since $A'A''$ is a normal line to GK, thus

$$x_{A''} = y_{A''} \tan \rho \tag{12}$$

$$y_{A''} = \frac{h \tan \rho + b \cos \rho - \sqrt{b \sin \rho \, (2h - b \sin \rho)}}{1 + \tan^2 \rho}. \tag{13}$$

In total, there are four yield lines to be considered which are GK, EL, HN, and FM with each length is b, like the width of the undeformed web. The energy absorbed in the complete mechanism becomes

$$\begin{aligned} W_5 &= W_{GK+EL+HN+FM} \\ &= 4 \cdot m_p \cdot b \arctan \left(\frac{z_A}{\sqrt{(h - x_{A''})^2 + (y_{A''} - y_B)^2}} \right). \end{aligned} \tag{14}$$

The energy absorbed by the four top half travelling hinge lines is equal to the area swept by the yield line multiplying by the mean curvature and fully plastic bending moment, m_p, and by taking z_A and h, it gives

$$W_6 = 4m_p \frac{h}{r}\Big(b\sin^2\rho - h\sin\rho + \sqrt{b\sin\rho(2h - b\sin\rho)}\cos\rho\Big). \tag{15}$$

Here, r is the radius of curvature that decreases slowly during deformation and Kecman (1983) [1] assumed empirically

$$r = r(\theta) = \left(0.07 - \frac{\theta}{70}\right)h. \tag{16}$$

The above expression falls within the acceptable range that is $r = \left(\frac{0.07}{0.06}\right)h$ if only $0 \leq \theta \leq 40°$. Similarly, for the four bottom half travelling hinge lines, assume that the curvature varies linearly or decreases rapidly within the lower half along KA with a distance l_k from K. The radius decreases slowly from flat web until becoming approximately equal to the *r* of GA at point A. Using hyperbolic function, such variation can be approximated to become

$$r_{KA} = \frac{KA}{l_k}r \tag{17}$$

where l_k is the rolling distance from K to A. Since the rolled length at A is equal to z_A, and *KA* varies linearly and gives

$$l_r = \frac{l_k}{KA}z_A. \tag{18}$$

The total energy absorbed along KA becomes

$$W_{KA} = \int_0^{KA} 2m_p \frac{l_r}{r_{KA}}\,\mathrm{d}l_k = \frac{2m_p z_A KA}{3r} \tag{19}$$

The distance KA is:

$$KA = \sqrt{h^2 + y_B^2 + z_A^2} \tag{20}$$

hence,

$$W_7 = W_{KA+LA+NJ+MJ} = \frac{8}{3}m_p \frac{z_A}{r}\sqrt{h^2 + y_B^2 + z_A^2}. \tag{21}$$

Here, y, z_A, h, and r have already been defined previously.

The Tension Lips and Closed-plate

The tension flange is free from concave formation; therefore, only bending along yield lines on the lips (OK, PL, MQ and NR) and plate (OR and PQ) can take place. The undeformed sections rotate relatively along yield lines OR and PQ at $\rho = \theta/2$, and triangle AKL and JMN rotate about lines KL and MN at $\xi = \arctan(z_A/y_A)$. The summation of energy absorbed becomes

$$\begin{aligned} W_8 &= W_{OK+PL+MQ+NR} + W_{OR+PQ} + W_{KL+MN} \\ &= 2m_p\left(a\rho + 4l\rho + 2h \arctan\left(\frac{z_A}{y_A}\right)\right) \end{aligned} \tag{22}$$

where z, h and $y_A - y_B$ are known.

The Total Energy Absorbed

The total energy absorbed is the summation of all the eight energy components. It can be expressed as a sum,

$$W(\theta) = \sum_{1}^{8} W_i(\theta). \tag{23}$$

The Theoretical Variation of the Hinge Moment

The effect of variation on the parameters and how the function reacts toward changes cannot be investigated by Equation (23). Differentiation can be used to study the variation of the hinge moment $\mathrm{M}(\theta)$ in a form,

$$\mathrm{M}(\theta) = \frac{\mathrm{dW}(\theta)}{\mathrm{d}\theta}. \tag{24}$$

Though Equation (24) is possible to derive, the resulting formula shall be too complex and impractical to be applied. It can possibly be solved using numerical approach by taking a small increment $\Delta\theta$.

$$\mathrm{M}(\theta) = \frac{\Delta\mathrm{W}(\theta)}{\Delta\theta} = \frac{\mathrm{W}(\theta + \Delta\theta) - \mathrm{W}(\theta)}{\Delta\theta}. \tag{25}$$

Equation (25) produces a theoretical $M - \theta$ curve from discrete points. The moment $\mathrm{M}(\theta)$ shall satisfy the condition below, where $M_{\max}$ is the maximum bending strength of the section.

$$\mathrm{M}(\theta) \leq M_{\max} \tag{26}$$

MATLAB Programming

For solving Equation (25), MATLAB for numerical computation was used and a program for the calculation was developed. The input data for MATLAB program is listed in Table 1.

Table 1: Matlab input measurements

Input	Symbols	Input	Symbols
Yield Stress	σ_y	**Web width**	W_w
Segment rotation	θ	**Lip**	W_l
Half rotation	ρ	**Radius of curvature**	r
Plastic bending moment	m_p	**Shell thickness**	t
Flange width	W_f	**Half hinge length**	h

Background of the Development of the FEA Model to Simulate Pure Bending

Model Geometry, Material Model, and Finite Element Mesh

Model geometry, material model, and FE meshing procedures follow the Part I [7] of this study. According to presimultion, the portion where the bending collapse is expected to occur was modeled with fine mesh (2 x 2 mm^2) and the rest with coarse mesh (5 x 2 mm^2) as shown in Figure 5.

Loading, Interaction, and Boundary Condition

The closed-hat-section beam lies flat on xz plane and longitudinally parallel to z axis. Both its opening sections were constrained to a rigid plate built up by R3D4 elements. The farthest rigid plate from refined mesh was fully constrained and another was made to rotate about beam's center with genuine rotation. Due to mirror symmetry, boundary conditions along free edges of beam are applied symmetrically constraining U1, UR2, and UR3. Both connectors and step time follow Part I [7] of this study.

Validation Results of the Theoretical Model Subject to Pure Bending

Moment-rotation curves for each section are plotted in Figure 6. The moment carrying capacity decreases dramatically as the plastic hinge rotation angle increases. Only simulation results indicate elastic deflection but theory does not start from zero and seems as if the elastic region has been subtracted. It

can actually start from the maximum bending strength which is governed by elastic buckling of the compression flange [8]. Due to the involvement of highly implicit nonlinear equation, it was not defined in the MATLAB. Both Kecman [1] and present simulation agree well as shown in Figure 6 and 7.

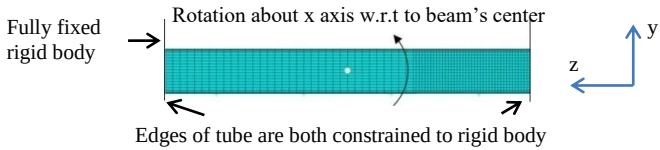

Figure 5: A FE mesh of the half model subject to pure bending

Table 2: Sections dimension and measured values

Section	Dimension (mm)			W_f/t	W_f/W_w	H (mm)
	W_f	W_w	W_l			
S1	60	30	30	60	2.00	8.00
S2	60	30	20	60	2.00	8.00
S3	100	30	30	100	3.33	8.00
S4	30	50	30	30	0.60	18.00

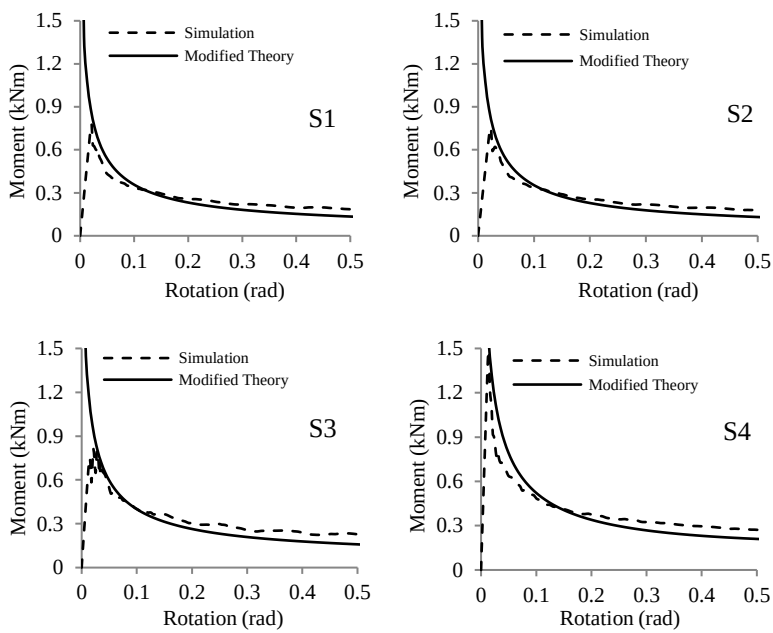

Figure 6: Moment-rotation results from simulation and calculated theory

Conclusion

The theoretical bending collapse mechanism of the closed-hat-section beam based on Kecman [1] has been presented. The theoretical expression of bending moments was derived based on energy dissipation mechanism of stationary hinge lines, rolling hinge lines, and stretched walls. FE method was employed to validate the accuracy of the modified theory. Results show that the theoretical bending collapse of the beam presented in this paper can describe the collapse process accurately. The calculated moment-rotation curves also show good agreement with simulation results. Therefore, the modified theory was successfully validated.

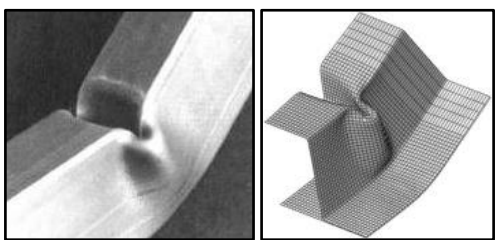

(a) (b)

Figure 7: (a) Kecman [1] collapse model and (b) present simulation (S4)

Acknowledgement

Deep gratitude to the Ministry of Education, Malaysia (MOE) and IRMI of Universiti Teknologi MARA (UiTM) for funding this research under Research Acculturation Grant Scheme (RAGS).

References

[1] D. Kecman, "Bending collapse of rectangular and square section tubes," Int J Mech Sci 25 (9), 623-636 (1983).

[2] S. J. Cimpoeru and N. W. Murray, "The large-deflection pure bending properties of a square thin-walled tube," Int J Mech Sci 35 (3-4), 247-256 (1993).

[3] T. Wierzbicki, L. Recke, W. Abramowicz, T. Gholami, and J. Huang, "Stress profiles in thin-walled prismatic columns subjected to crush loading-II. Bending," Comput Struct 51 (6), 625-641 (1994).

[4] T. H. Kim and S. R. Reid, "Bending collapse of thin-walled rectangular section columns," Comput Struct 79 (20), 1897-1911 (2001).

[5] W. Chen, "Experimental and numerical study on bending collapse of aluminum foam-filled hat profiles," Int J Solids Struct 38 (44), 7919-7944 (2001).

[6] M. Bambach, G. Tan, and R. Grzebieta, "Steel spot-welded hat sections with perforations subjected to large deformation pure bending," Thin-Walled Structures 47 (11), 1305-1315 (2009).

[7] H. Hashim, A. R. A. Ghani, and W. Kuntjoro, "Bending Collapse of Closed-hat-section Beams. Part I: Development and Validation of Finite Element Models," unpublished (2016).

[8] D. Kecman and G. D. Suthurst, "Theoretical determination of the maximum bending strength in the car body components," International Conference on Vehicle Structures, July 16-18 (1984).